Investigating casein gel structure during gastric digestion using ultra-small and small-angle neutron scattering

Meltem Bayrak, Jitendra Mata, Jared K Raynes, Mark Greaves, Jacinta White, Charlotte E Conn, Juliane Floury, Amy Logan

Journal of Colloid and Interface Science 594 (2021) 561–574

Contents lists available at ScienceDirect

Journal of Colloid and Interface Science

journal homepage: www.elsevier.com/locate/jcis

Regular Article

Investigating casein gel structure during gastric digestion using ultra-small and small-angle neutron scattering

Meltem Bayrak [a,b,*], Jitendra Mata [c], Jared K. Raynes [a], Mark Greaves [d], Jacinta White [d], Charlotte E. Conn [b], Juliane Floury [e], Amy Logan [a]

[a] CSIRO Agriculture and Food, 671 Sneydes Road, Werribee, Victoria 3030, Australia
[b] School of Science, STEM College, RMIT University, 124 La Trobe Street, Melbourne, VIC 3000, Australia
[c] Australian Centre for Neutron Scattering, Australian Nuclear Science and Technology Organisation, Lucas Heights, NSW 2234, Australia
[d] CSIRO Manufacturing, Bayview Avenue, Clayton, VIC 3168, Australia
[e] STLO, INRAE, Institut Agro, 35042 Rennes, France

HIGHLIGHTS

- The first study to monitor gastric devolution of casein gels using USANS and SANS.
- Gels prepared in D_2O exhibit earlier onset of gelation, are firmer yet more brittle compared to H_2O.
- Rennet-induced gel structure is sensitive to the acidic environment of the stomach.
- Pepsin induces micelle swelling and promotes higher levels of protein digestion in the stomach.
- Acidification and shear govern early gastric digestion kinetics.

GRAPHICAL ABSTRACT

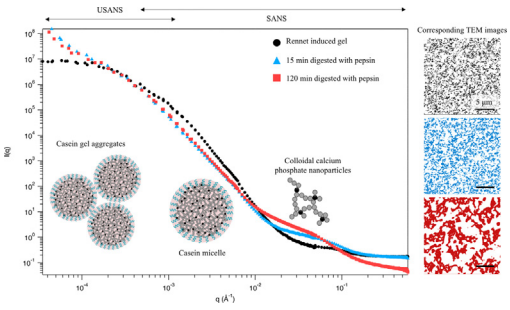

ARTICLE INFO

Article history:
Received 27 July 2020
Revised 24 February 2021
Accepted 15 March 2021
Available online 19 March 2021

Keywords:
Protein dairy protein gel
Casein
Structure
Digestion
Neutron scattering
Electron microscopy
Solubilised protein

ABSTRACT

This study aimed to understand the structural devolution of 10% w/w rennet-induced (RG) and transglutaminase-induced acid (TG) gels in H_2O and D_2O under *in vitro* gastric conditions with and without pepsin. The real-time devolution of structure at a nano- (e.g. colloidal calcium phosphate (CCP) and micelle) and micro- (gel network) level was determined using ultra-small (USANS) and small-angle neutron scattering (SANS) with electron microscopy. Results demonstrate that gel firmness or elasticity determines disintegration behaviour during simulated mastication and consequently the particle size entering the stomach. Shear of mixing in the stomach, pH, and enzyme activity will also affect the digestion process. Our results suggest that shear of mixing primarily results in erosion at the particle surface and governs gel disintegration behaviour during the early stages of digestion. Pepsin diffusivity, and hence action, occur more readily in the latter stages of gastric digestion via access to the particle interior. This occurs via the progressively larger pores of the looser gel network and channels created within the larger, less dense casein micelles of the RG gels. Gel firmness and brittleness were greater in the D_2O samples compared to H_2O, facilitating gel disintegration. Despite the higher strength and elasticity of RG compared to TG, the protein network strands of the RG gels become more compact when exposed to the acidic gastric environment with comparatively larger pores observed through SEM imaging.

* Corresponding author at: CSIRO Agriculture and Food, 671 Sneydes Road, Werribee, Victoria 3030, Australia.
E-mail addresses: meltem.bayrak@csiro.au (M. Bayrak), jitendra.mata@ansto.gov.au (J. Mata), jared.raynes@csiro.au (J.K. Raynes), mark.greaves@csiro.au (M. Greaves), jacinta.white@csiro.au (J. White), charlotte.conn@rmit.edu.au (C.E. Conn), juliane.floury@agrocampus-ouest.fr (J. Floury), amy.logan@csiro.au (A. Logan).

https://doi.org/10.1016/j.jcis.2021.03.087
0021-9797/

This led to a higher degree of digestibility in RG gels compared to TG gels. This is the first study to examine casein gel structure during simulated gastric digestion using scattering and highlights the benefits of neutron scattering to monitor structural changes during digestion at multiple length scales.

1. Introduction

The delivery of food nutrients and their benefits to the consumer are determined, to a large extent, by the microstructure of the food within which they are contained [75,80,82,95]. A comprehensive understanding of the role of food microstructure to control nutrient release during digestion therefore offers a unique opportunity to design food structures targeted towards a specific health function. Proteins can adopt a wide range of structures at both the micro- and nano-scale. The functional properties of most dairy-based products, including cheese and yoghurt, are governed by the protein–protein interactions of the casein micelles. Casein proteins, which represent nearly 80% of the proteins found in cow's milk, have been extensively studied as a model system for gel formation or as a food system [12,26,39].

Casein micelles consist of four main types of phosphoproteins (αs1-, αs2-, β-, κ-casein) linked by colloidal calcium phosphate (CCP), with κ-casein exclusively protruding from the micelle surface effectively creating a "hairy layer" (Fig. 1). The casein micelle structure has been described previously using small-angle x-ray scattering (SAXS) and small-angle neutron scatting (SANS) techniques, and defined according to a number of different models [11,24,36,40,41;56,61,65].The structure of the casein micelle is sensitive to environmental changes such as pH, temperature, and ionic strength, and a reduction in stability results in self-aggregation, network formation and inevitably the development of semi-solid dairy gels [3,23,39,98]. Rennet-induced gel (RG) and transglutaminase-induced acid gel (TG) network structures were selected in this study as representative of major dairy product categories (Fig. 1). Rennet is the enzyme that catalyses aggregation of most cheeses by selective hydrolysis of κ-casein at the micelle surface, reducing the electrostatic and steric stability of the individual micelles [22,25]. Acid-induced milk gels, such as yoghurt, are formed by adjusting the pH to the isoelectric point of the casein, neutralizing the surface charge of the micelles, leading to aggregation through mainly hydrophobic interactions [55]. The acid gel structure may also be modified via the introduction of new covalent bonds [90], such as TG, created through the covalent cross-linking between glutamine and lysine residues of the aggregated casein proteins [30,84]. These different modes of casein gelation lead to the formation of unique nano- and microstructures which influence the functional properties of the gel, such as gel strength, elasticity, brittleness, resistance to shear and overall physical stability to phase separation [48,63,67,76,97,101].

Once food passes into the stomach, complex enzymatic, physical (peristaltic mixing and shear) and chemical (pH decrease and ionic composition) processes occur that influence digestion [10]. The pepsin enzyme catalyses the partial hydrolysis of proteins in the stomach and is responsible for around 20% of total protein digestion that occurs after a food is eaten [31,66]. As such, the extent of protein hydrolysis that occurs in the stomach under gastric conditions is limited compared to the intestinal phase [46,75]. Nevertheless, gastric digestion is important as digestion kinetics influence gastric emptying rates, which in turn influence satiety

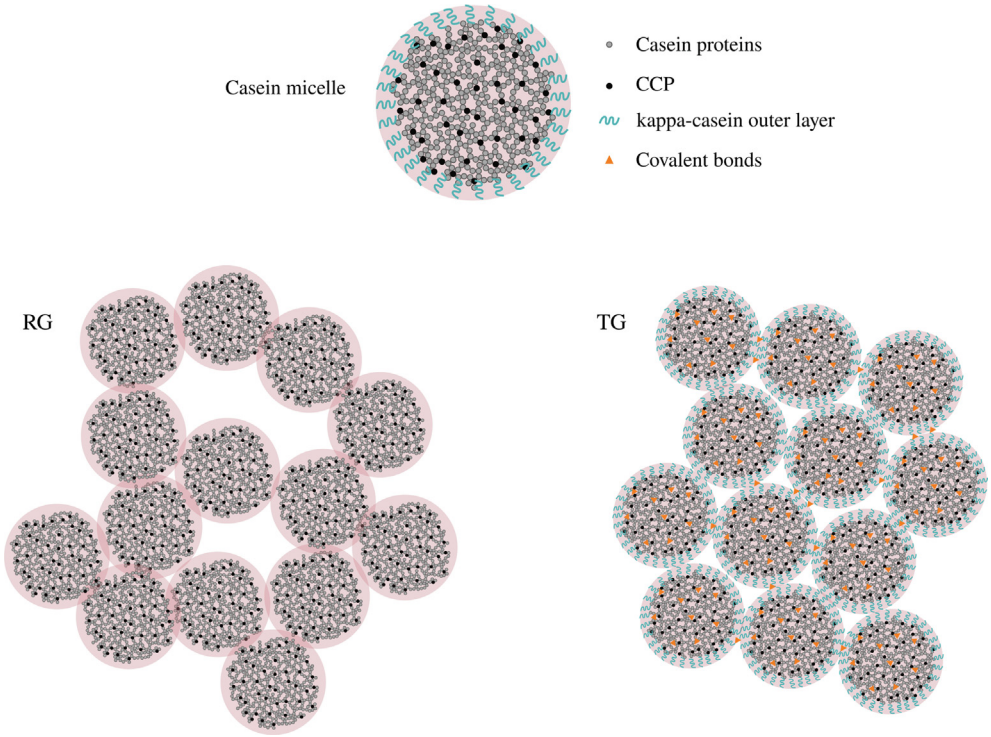

Fig. 1. Schematic representation of an individual casein micelle structure (top), and the protein network of the rennet-induced gel (RG) and transglutaminase-induced acid gel (TG) structures (bottom) demonstrating the porosity and irregularity. CCP = colloidal calcium phosphate.

and can control nutrient absorption in the small intestine and the subsequent physiological responses [10,88]. Understanding disintegration kinetics of protein food matrices in the stomach is essential to controlling food processing conditions to promote optimum breakdown.

Several studies have demonstrated the impact of dairy gel structures on disintegration kinetics of the protein gel particles [33], the amino acid bioavailability [8] and pepsin diffusion coefficients within casein gels [96] upon *in vitro* gastric digestion. Floury, et al. [33] have shown pepsin to have a limited penetration depth within compact protein aggregates as a result of the reduced accessibility of pepsin to its substrate, and instead suggest that hydrolysis of proteins during gastric digestion mainly occurs at the surface of a gel particle. However, the mechanism of how a dairy gel disintegrates over a hierarchy of length scales (nano- to micro) during digestion is still to be elucidated. Moreover, the individual contribution of the different components of gastric digestion, namely, mechanical shear, enzymatic hydrolysis and the effect of acidification, are yet to be determined. Pasquier, et al. [81] reported the first small-angle neutron scattering (SANS) study to monitor changes in food structure during simulated *in vitro* gastric and intestinal digestion with different vegetable (cruciferin and napin) protein gels. Herein, we focus on the influence of a simulated gastric environment (mechanical shear and acidification) with and without pepsin on the devolution of the gel structure of RG and TG model casein gels using SANS and ultra-small angle neutron scattering (USANS) in combination with scanning (SEM) and transmission electron microscopy (TEM) to characterise the initial gel structure and subsequent changes in structure under the simulated gastric environment. Control experiments were conducted without pepsin to address the influence of acidification and shear of mixing on the protein gels disintegration in isolation. The wide q-range covered by the combination of SANS and USANS allows us to track the devolution of the casein micelle structure across multiple length scales covering a size scale from protein-protein aggregation (~5 μm) to the CCP nanoclusters located within the interior of the micelle (~5 nm). To the knowledge of the authors, this is the only study using time-resolved USANS and SANS in combination to investigate the structural devolution of casein gels throughout simulated gastric digestion.

Moreover, heavy water (D_2O) is a common solvent for neutron scattering experiments, and this is the first study to examine the structural changes of a gel prepared and analysed in both in H_2O and D_2O during simulated *in vitro* digestion.

2. Materials and methods

2.1. Materials

Micellar casein powder (PRODIET 85B) (MCP) was purchased from Ingredia (Arras, France). It's protein content was confirmed as 82.41 g per 100 g dry solid according to the Dumas method (AOAC method 992.15, 2005) using a LECO TruMac Nitrogen analyser (Leco Corp., St Joseph, MI, USA). Transglutaminase (ACTIVA WM; 100 U g^{-1}) was kindly supplied by Ajinomoto Foods Europe, Japan. Chymosin, the primary enzyme in rennet (CHY-MAX® Plus; 200 IMCU mL) was purchased from Chr Hansen Bayswater, Victoria (Australia). Pepsin from porcine gastric mucosa (P6887), deuterium oxide (D_2O; 151882), pepstatin A (P5318), D-(+)-Gluconic acid δ-lactone (G4750), haemoglobin from bovine blood (H6525) and all other chemicals were purchased from Sigma-Aldrich, Inc (St. Louis, MO, USA). The standardised pepsin activity assay (EC 3.4.23.1) was performed in triplicate using haemoglobin as a substrate in both H_2O and D_2O [13]. Milli-Q water and analytical grade chemicals were used for all experiments.

2.2. Methods

2.2.1. Preparation of solubilized micellar casein solution and gels

The MCP 10% (w/w) solution was freshly prepared for each gel and experiment by rehydrating the powder into H_2O or D_2O with stirring in a water bath (50 °C). This concentration was selected on the basis of a preliminary SAXS experiment that examined RG and TG gels preparing 5, 7.5, 10% (w/w) MCP solutions. The gels prepared from the 10% (w/w) solution presented the best balance between acquisition time to collect data and reduction of background scattering, providing opportunity for more structuring factors to emerge, allowing for better differentiation between the H_2O and D_2O samples while having a closer appearance to a pot set type yoghurt and rennet curd typical for cheddar hard-type production (data not shown). Sodium azide (0.02%(w/w)) was added to the solution to prevent microbial growth and the solution was homogenised using an ultra-turrax (10,000 rpm, 5 min). The solution was stirred (6 h, 50 °C), homogenised for a second time (10,000 rpm, 5 min) and stirred overnight at room temperature. The degree of solubilisation (98.07 ± 3.29% for H_2O and 96.45 ± 2. 34% for D_2O) of the warmed solution (40 °C, 30 min) was calculated the following morning [15,71]and confirmed by particle size analysis (Mastersizer2000, Malvern Instruments, England) using a refractive index of 1.462 for the casein, 1.333 for H_2O and 1.328 for D_2O, according to the method of SG Anema, Pinder, Hunter, and Hemar [6].

The pD of the MCP solution in D_2O was adjusted to the same pH of the MCP solution in H_2O, using the pD = pH + 0.4 formula [17]. For the preparation of RG and TG, the solutions were warmed to 32 °C or 40 °C respectively, for 1 h with stirring. The pH or pD was adjusted to 6.5 using 1 M HCl or DCl for RG gel preperation. Chymosin (200 IMCU mL^{-1} stock, 0.03 IMCU mL^{-1} final concentration) for RG or transglutaminase powder (5U g^{-1} final concentration) and 1.1% (w/w) glucono-∂-lactone (GDL) for TG was added to the MCP solution stirred at 700 rpm, for 30 s. The MCP-rennet or MCP-TGase-GDL solution was poured into specially prepared plastic tubing (sealed bottom), returned to the water bath (32 °C or 40 °C) and allowed to gel for 60 min. For TG, solutions with the same pH and pD values were warmed to 40 °C for 1 h with stirring. Digestion experiments were performed within 24 h of gel preparation. The pH of the final TG and RG samples were 5.66 ± 0.09 and 6.57 ± 0.07 for H_2O and 5.72 ± 0.05 and 6.18 ± 0.13 for D_2O respectively. Gels were freshly prepared on at least two occasions; RG prepared with H_2O (RG-H_2O), RG prepared with D_2O (RG-D_2O), TG prepared with H_2O (TG-H_2O) and TG prepared with D_2O (TG-D_2O).

2.2.2. Rheological characterisation of casein gels

Rheological characterisation of the casein gels was conducted using an Anton Paar-Physica rheometer (MCR 302, Anton Paar Physica, Physica Meßtechnik GmbH, Stuttgart, Germany) equipped with a CC27 cup and bob geometry system according to the method of [58]. In brief, the gelation properties were followed by monitoring the storage (G′, Pa) and the loss modulus (G″, Pa) at a frequency of 1 Hz. The final value of G′ ($G'_{60\ min}$), G″ ($G''_{60\ min}$) and tan δ (the loss tangent, G″/G′) were recorded after 60 min from rennet/transglutaminase addition. The onset of gelation (min) was defined as the time at which the G′ first reached 0.05 Pa [59]. The gels were brought to room temperature and a frequency sweep was performed where G′ and G″ were measured as a function of frequency from 0.1 to 10 Hz at a constant strain of 0.1% at 25 °C. The ratio between G′ and frequency is related to the nature and strength of a gel [4]. Rheology experiments were carried out in triplicate for RG and TG gels prepared in either H_2O or D_2O using freshly prepared MCP solution on each occasion.

2.2.3. In vitro gastric digestion with pepsin and control experiment without pepsin

The *in vitro* gastric digestion experiment with pepsin and control experiments without pepsin were conducted in order to separate the effect of the enzymatic action of pepsin from the effect of acidification and mixing during digestion. Freshly prepared RG and TG gels were digested in either H_2O and D_2O on at least two different occasions according to Brodkorb, et al. [13]. Digestive fluids (simulated salivary fluid (SSF, pH/pD 7.0) and simulated gastric fluid (SGF, pH/pD 3.0) were prepared with sodium bicarbonate replaced by sodium chloride in order to avoid unwanted pH drifts [13]. To mimic in-mouth mastication, the casein gels (10 g) were removed from the specially prepared plastic tubing by applying sequential pressure between fingers to replicate the action in the mouth, where the tongue presses against the top pallet before swallowing, and mixed with SSF (10 mL). The gel-SSF mixture was placed in a water bath (37 °C) and stirred at 200 rpm. After 2 min, SGF (16 mL) and pepsin (2 mL, 2000U mL^{-1} in final digesta) or an equal volume of H_2O or D_2O were added. HCl or DCl (5 M) and H_2O or D_2O were added to produce a final volume of 40 mL at a pH or pD of 3.0. The *in vitro* gastric digestion continued at 37 °C with stirring (200 rpm) for up to 120 min. The pH or pD was measured every 5 min and adjusted to maintain a constant pH at 3.0. Pepstatin A (400 μL, 0.5 mg mL^{-1}) was added as a protease inhibitor to stop the enzyme reaction. An equal volume of H_2O or D_2O was added for the control experiments where pepsin was not added. The size of the gel particles after simulated mastication (mixed with SSF for 2 min at 200 rpm) were imaged immediately in triplicate measurements for each gels using a ColourView III camera fitted with an Olympus OM system 50 mm f1.4 lens via an Olympus to C mount adapter (Olympus, Tokyo, Japan) and the size of particles in binary images were analysed by ImageJ [1].

2.2.4. Ultra-Small-Angle (USANS) and Small-Angle (SANS) neutron scattering

The SANS and USANS measurements were performed on the 40 m QUOKKA [103] and KOOKABURRA [87] beamlines respectively at the OPAL reactor (Lucas Heights, NSW, Australia). The SANS measurements were performed with camera lengths of 2, 12 and 20 m to cover a large q-range (7×10^{-4} $Å^{-1}$ to 0.5 $Å^{-1}$) and overlap with USANS data (3.5×10^{-5} $Å^{-1}$ to 0.008 $Å^{-1}$) were performed using a Bonse-Hart instrument. The samples were loaded into demountable sample cells with a path length of 1 mm. A thermally controlled sample charger was used to control the sample temperature to 37 °C. The experimental USANS data were de-smeared using the Lake algorithm incorporated in NIST USANS macros and subsequently merged with SANS data [45] while SASView was used for data interpretation [28].

The models used in the literature to analyse scattering data are based on a number of assumptions around the shape, polydispersity and interactions of casein micelles. In the current study, the scattering curves of the casein gels and their digesta demonstrate three distinctive features that were fitted by separate models including the power law, Guinier (Guinier, Fournet, & Yudowitch, 1955), triaxial ellipsoid [32] and Gaussian peak models, to provide a comprehensive understanding of the hierarchical structure over the varying length scales. These regions are represented in Fig. 6, as follows; region[1] = ultra-low q (<0.0001 $Å^{-1}$), region[2] = low and intermediate q (0.001–0.01 $Å^{-1}$), and region[3] = high q (0.05> $Å^{-1}$), and correspond to a length scale of < 6.28 μm [1], 413 nm – 41.3 nm [2], and > 12.5 nm [3], respectively. The q-values on the x-axis define the real space structural distances (d), where $d = 2\pi/q$. Contrast variation was achieved in this work using both H_2O and D_2O. This is a common approach used in neutron scattering to observe different components of a system based on differential scatter between hydrogen and deuterium. The H_2O and D_2O solvent systems were used in this experiment for the purpose of accentuating the CCP nanoclusters located within the micelle structure in the high-q region [3].

The power law exponent for each gel (Table 3), was calculated from the slope of the ultra-low q region [1]. The power law applied for large aggregates accounts for any interparticle interaction in the casein micelle range. However, it is noted that the q-range available for the power law fit was limited which could influence the accuracy of results. In accordance with established theory, the low and intermediate q region [2] corresponds to a size scale around 200 nm, and represents the form factor scattering of polydisperse casein micelles. A Guinier approximation was applied to estimate the size of casein aggregates fused together to form network strands via the radius of gyration (Rg) [35]. The radius of gyration is referred to as 'apparent Rg' in this study to incorporate the underlying inter-particle interaction factor in the Guinier region, where the relative change in structure was considered as the focus of this study as opposed to quantitative values. Based on these apparent Rg results and the appearance of micelle shapes from TEM images, a triaxial ellipsoidal model was applied using the equation deducted from Shah, et al. [91].

The inflection in the high-q region [3] relates to the interior of the casein micelles and with a length scale of approximately 20 nm in size (Fig. 8), where the CCP nanoclusters are spaced at distances of around 18 nm from each other, with a radius of approximately 2.4 nm [104]. The inflection observed near 0.0035 $Å^{-1}$allows for the estimation of partial CCP dissolution, where a decrease in neutron signal equates to greater dissolution. Using the height, position and width of the inflection, the effect of the *in vitro* digestion can be revealed through the qualitative differences between samples, where a wider inflection indicates less dense CCP nanoclusters, and shift to a smaller q suggests an increase in CCP spacing.

2.2.5. Scanning and transmission electron microscopy

Both an SEM and TEM approach were used to visualise the casein gel and digesta samples collected over two different occasions. Samples were immediately fixed in 3% (w/v) glutaraldehyde overnight at 4 °C and washed three times in 0.1 M Sorensen's buffer (ProSciTech, Thuringowa, QLD ASOR68C) and left in PBS at 4 °C until analysis.

Samples for SEM were processed through HMDS using standard methodology as outlined in [9]. The samples were imaged using a Zeiss Sigma Field Emission Scanning Electron Microscope (Zeiss, Jena, Germany) operated in the secondary electron (SE) mode, at 3 kV.

For TEM, samples were processed through a Procure 812 resin using standard methodology as outlined in White, Werkmeister, Hilbert, and Ramshaw [102]. Micrographs were imaged using a Tecnai 12 Transmission Electron Microscope (FEI, Eindhoven, The Netherlands) at an operating voltage of 120 kV. Images were recorded using a FEI Eagle 4kx4k CCD camera and AnalySIS v3.2 camera control software (Olympus). Ten representative images were taken at a magnification of x1650. Following adjustment of images to 32-bit grayscale of 4090 × 4090 pixels, the black-top hat filter was used to enhance casein gel network and Otsu thresholding algorithm to convert into binary image. Two different microstructural parameters were determined from binary images: the average area density, i.e. the ratio between the protein matrix area with respect to the total area of the image (dimensionless), and the size distribution of particle aggregates (μm) using the procedure previously developed by J. Silva, Legland, Cauty, Kolotuev, and Floury [92], described in Thevenot, et al. [96] and implemented in FIJI software with MorphoLibJ, Granulometry, Geodesics plugins [52,53,54].

2.2.6. Release of soluble protein

This approach compared the amount of solubilised protein measured as a percentage in the supernatant compared to the total protein. The digesta, containing gel particles and gastric liquid, were centrifuged (500 rpm, 5 min, 25 °C) and the protein content of the supernatant (% nitrogen × 6.38) was measured (AOAC method 992.15, 2005) using a LECO TruMac Nitrogen analyser (Leco Corp., St Joseph, MI, USA). Analysis was performed in triplicate for gels prepared on at least two different occasions.

2.2.7. Release of peptides and amino acids

The O-phthaldialdehyde (OPA) method described in Nielsen, Petersen, and Dambmann [74] was used to measure levels of low-molecular weight peptides and amino acids smaller than 10 kDa solubilised in the supernatant [60]. The digesta supernatant were filtered through a Vivaspin 20 centrifugal filter (Sartorius AG, Gottingen Germany) by centrifugation (10,000 g, 30 min, 4 °C) and OPA solution was prepared as described by Lorieau, et al. [60]. Glycine standard (0.250 mmol/L) and 1:40 diluted samples (50 uL) were added in a flatbottom 96-well microtiter plate (Greiner Bio-One, Courtaboeuf, France). The OPA solution (200 uL) was added to each well and shaken for 5 min at 600 rpm. After 20 min incubation at 25 °C, 340 nm excitation and 450 nm emission was automatically measured using a FLUOstar Omega microplate reader (BMG Labtech, Ortenberg, Germany). Absorbance readings were quantified using a glycine calibration curve and the peptide release percentage calculated compared to the total number of hydrolysed peptide bonds per protein equivalent, where casein is equal to 8.2 mmol g^{-1} protein [2]. Analysis was performed in triplicate for gels prepared on at least two different occasions.

2.3. Statistical analysis

Data were analysed for statistical differences between samples by one-way analysis of variance (ANOVA) using RStudio v3 software (RStudio™, Boston, MA, USA) with "TukeyHSD" function. To measure differences in mean values, a p value < 0.01 was considered to be statistically significant.

3. Results

3.1. Rheological behaviour

The gelation onset, storage (G′) and loss (G′′) moduli, and tan δ after the 60 min gelation protocol are shown in Table 1. A clear difference between rheological properties in response to solvent (H_2O or D_2O) and gelation type (RG and TG) was observed. The dynamic storage and loss moduli were found to rapidly increase immediately following the induction period, denoted by the gelation onset, before tending towards a plateau as described previously for rennet-induced gels [44,58,59,62,67] and acid gels that were subsequently cross-linked via a transglutaminase-induced reaction [42;85,86;93]. After 60 min gelation, the casein gels formed with RG and prepared in both D_2O and H_2O were significantly firmer than TG, with G′, around 6–8 times higher. Similarly, casein gels formed in D_2O were firmer than H_2O with an earlier gelation onset. However, overall the tan δ values (the ratio of viscous to elastic properties) were 3.4 or higher for all gels, indicating weak gel behaviour. The least elastic behaviour was observed for TG-D_2O, whereas the lower tan δ for RG-H_2O indicates higher gel elasticity.

This 60 min gelation protocol was immediately followed by a frequency sweep to investigate the large deformation behaviour of the gels. With the increasing frequency, more bonds are relaxed leading to an increase in G′ (Fig. 2) and G′′ (data not shown).

3.2. Particle size distribution of gels upon simulated mastication

Images representing the size of gel particles entering the stomach upon simulated mastication are shown in Fig. 3. The gel particles of RG and TG were sorted into 3 groups: large (>0.5 cm), medium (0.01–0.5 cm) and small (<0.01 cm) in diameter. The average size distribution of the large particles in RG and TG was between 0.6 and 2.6 and 1.0–2.6 cm, respectively. The RG-H_2O samples result in a narrow distribution of large particles only, with no medium sized particles observed. Medium sized particles of TG-H_2O and RG-D_2O had a median value of around 0.15 cm, while the medium sized particles for TG-D_2O were larger, at around 0.25 cm. All gels resulted in the formation of small particles (data not shown).

3.3. Microstructural properties

The network structure of the initial casein gels and their digesta (with and without pepsin) were visualised using SEM (Fig. 4) and TEM binary images, from which the aggregate area density (Table 2) and micelle aggregate size distribution (Fig. 5) were calculated using image analysis. The SEM images of the initial TG structure show a filamentous network of fine strands, packed into a dense cluster arrangement in which pore size seems visually similar (Fig. 4 C1&D1). In contrast, RG is composed of more irregular sized aggregates occurring across the network with larger pores (Fig. 4 A1&B1). This is in agreement with the TEM gel cross sections presented in Fig. 5 and reflects the differences in distribution span and average micelle particle size calculated from the TEM images. Analysis of the TEM images suggests a narrower particle size distribution in D_2O (Fig. 5 C&D) compared to gels prepared with H_2O (Fig. 5 A&B). The SEM images reveal that gels made with D_2O seem to present a finer and more homogeneous network structure with decreased porosity, leading to smaller pores, while H_2O gels tend to form a more robust and irregular structure (Fig. 4 A1-D1).

The effect of the acidic environment of the stomach on the casein gel microstructure is shown in the SEM images (Fig. 4). The digesta of control samples without pepsin after 120 min (Fig. 4 A5, B5, C5, D5) were influenced to a lesser degree compared to digestion with pepsin, from which the effect of pepsin in isolation can be inferred. The effect of the acidic gastric environment is most clearly observed in RG-H_2O digesta, characterised by large and thick aggregate clusters, larger pores and a higher area density

Table 1
The onset of gelation (min) for the 10% (w/w) casein gels, and the storage modulus (G′), loss modulus (G′′) and tan δ after 60 min gelation, for the; rennet-induced gel in D_2O (RG-D_2O); rennet-induced gel in H_2O (RG-H_2O); transglutaminase-induced acid gel in D_2O (TG-D_2O); and transglutaminase-induced acid gel in H_2O (TG-H_2O).

Gel type	Gelation onset (min)	$G'_{60\ min}$ (Pa)	$G''_{60\ min}$ (Pa)	tan δ
RG-D_2O	9.1 ± 0.1^{b}	1636.7 ± 75.7^{d}	459.7 ± 21.5^{d}	3.56 ± 0.01^{a}
RG-H_2O	14.6 ± 0.1^{d}	1183.3 ± 55.1^{c}	348.7 ± 14.0^{c}	3.39 ± 0.02^{a}
TG-D_2O	1.3 ± 0.4^{a}	504.0 ± 27.7^{b}	119 ± 10.4^{b}	4.24 ± 0.13^{b}
TG-H_2O	11.3 ± 1.1^{c}	210.0 ± 26.0^{a}	58.1 ± 8.3^{a}	3.62 ± 0.08^{a}

*All values are the mean of triplicate analyses ± the standard deviation. Values marked with different letters in the same column are significantly different across samples for gelation onset, G′, G′′ and tan δ (P < 0.01).

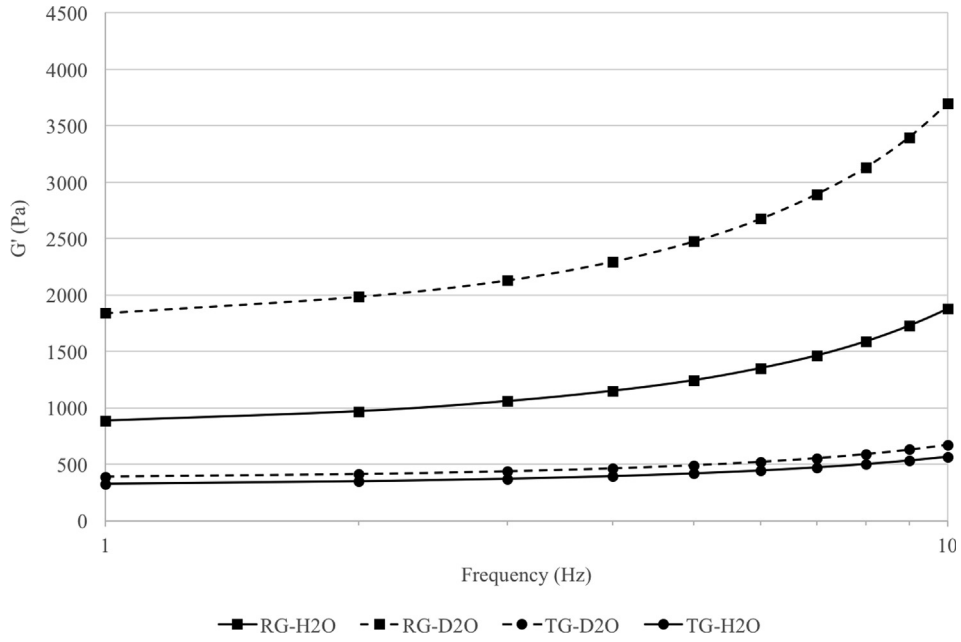

Fig. 2. Rheological properties as a function of applied frequency varying from 0.1 to 10 Hz at a constant strain of 0.1% to observe the time-dependent behaviour of the 10% (w/w) gels after the 60 min gelation followed by the simulation of storage conditions of gels for the: rennet-induced gel in D_2O RG-D_2O (– ■ –); rennet-induced gel in H_2O RG-H_2O (—■—); transglutaminase-induced acid gel in D_2O TG-D_2O (– ● –); transglutaminase-induced acid gel in H_2O TG-H_2O (—●—). The viscoelastic properties shows weak power-law behaviour with a plateau in G′ at lower frequencies and a small inflection upwards at the higher frequencies.

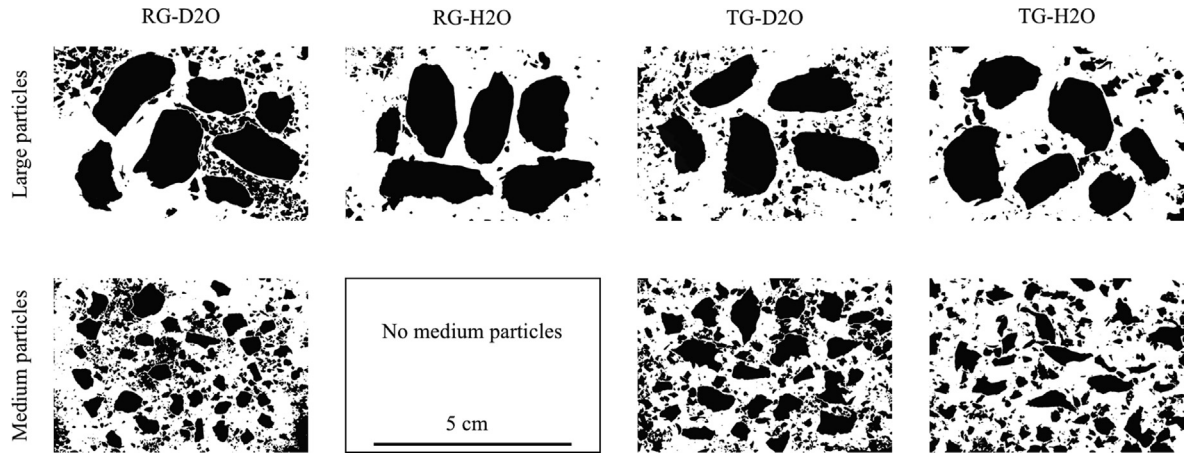

Fig. 3. Macro images that show the particle size distribution of the masticated 10% (w/w) casein gels in simulated saliva fluid (SSF) with mixing for 2 min at 200 rpm to replicate the oral phase protocol. No medium-sized particles were observed for RG-H_2O samples after mastication.

compared to the initial gel (Fig. 4 B-B5, Table 2). This also coincided with gel partial contraction and shrinkage observed for the RG samples, transforming into a more compact microstructure (Fig. 4 A2&B2, A4&B4), and believed to be associated with acid-induced syneresis previously demonstrated by Floury, et al. [33]. Exposure of TG to the acidic gastric environment results in an increase in area density in H_2O only (Table 2) and a limited change in protein network aggregation (Fig. 4 C4-C5, D4-D5).

This change was more pronounced in the presence of pepsin, with a higher degree of porosity and visible cavities observed after 120 min, especially in the RG samples (Fig. 4 A3, B3, C3, D3) where a more diffuse structure of longer aggregate strands, larger pores, and higher average area density (Table 2) are evident. This change was more pronounced in RG in H_2O compared to D_2O (Fig. 4 A3-B3), with less interactions between casein micelles, forming larger pore networks compared to D_2O. On the other hand, little difference in the gel particle microstructure was observed between TG prepared in either H_2O or D_2O and its digesta with or without pepsin (Fig. 4C1-D5, Fig. 4 C&D). Neither the casein micelle size distribution of TG-D_2O digested with pepsin nor the control experiment without pepsin changed over the 120 min period (Fig. 5 C), while there was a slight increase in particle size within the TG-H_2O subset when pepsin was present (Fig. 5 D).

3.4. SANS and USANS study of the initial gel and digesta

Experiments using USANS and SANS were performed on the casein gels and their digesta after 15 and 120 min under *in vitro* gastric conditions, with and without pepsin. The combined USANS and SANS spectra for the initial RG and TG gels in H_2O and D_2O prior to digestion are provided in Fig. 7 where the scattering behaviour of the three distinctive regions are presented, while Fig. 8 presents SANS spectra of initial gels and their digesta in the high q region. The microstructural information obtained from the

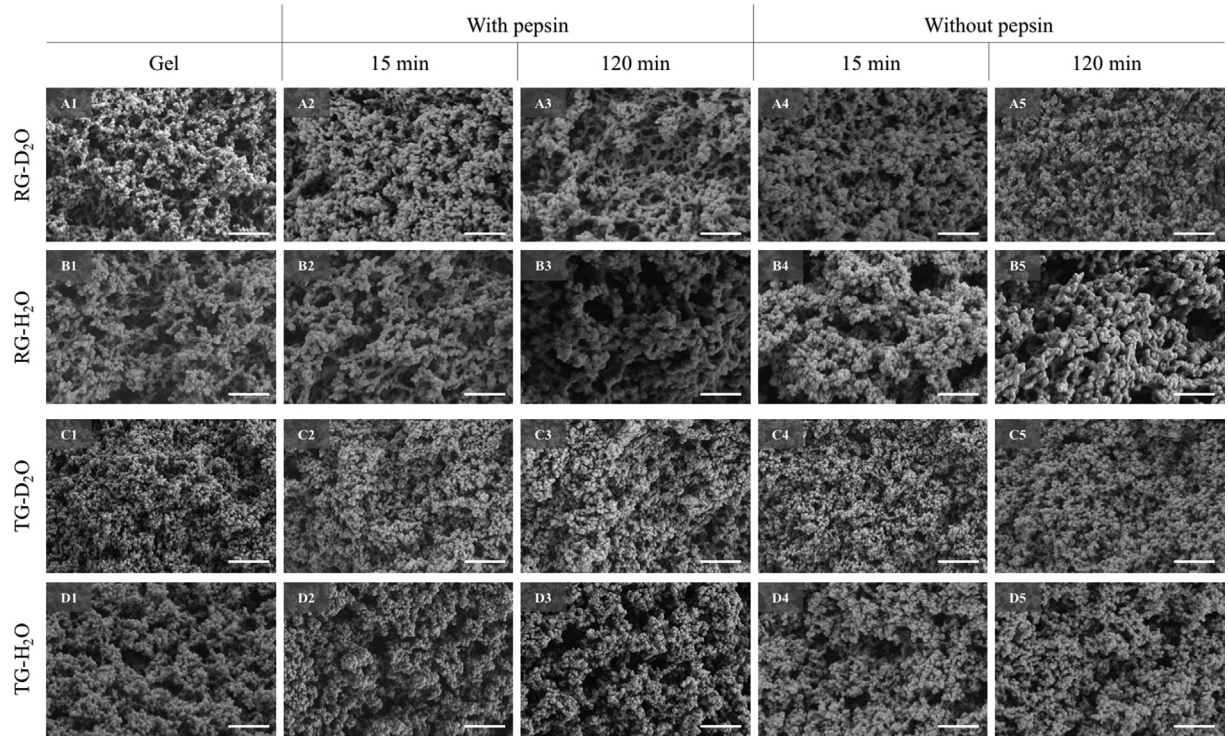

Fig. 4. Scanning electron microscopy (SEM) images of the initial 10% (w/w) casein gels and their digesta after 15 and 120 min obtained from experiments with and without pepsin, for the; (A1-A5) rennet-induced gel in D_2O (RG-D_2O); (B1-B5) rennet-induced gel in H2O (RG-H_2O); (C1-C5) transglutaminase-induced acid gel in D2O (TG-D_2O); and (D1-D5) transglutaminase-induced acid gel in H2O (TG-H_2O). Magnification 10,000X; Scale bars represent 2 μm.

Table 2
The average area density covered by casein protein aggregates for the initial 10% (w/w) casein gels and their digesta after 120 min obtained from experiments with (w) and without (w/o) pepsin and calculated from analysis of transmission electron microscopy (TEM) images, for the; rennet-induced gel in D_2O (RG-D_2O); rennet-induced gel in H_2O (RG-H_2O); transglutaminase-induced acid gel in D_2O (TG-D_2O); and transglutaminase-induced acid gel in H_2O (TG-H_2O).

Gel type	Average density
RG-D_2O initial gel	0.17 ± 0.01[a]
RG-D_2O 120 min w pepsin	0.41 ± 0.01 [d]
RG-D_2O 120 min w/o pepsin	0.34 ± 0.01[c]
RG-H_2O initial gel	0.23 ± 0.01[b]
RG-H_2O 120 min w pepsin	0.54 ± 0.01 [e]
RG-H_2O 120 min w/o pepsin	0.34 ± 0.01[c]
TG-D_2O initial gel	0.25 ± 0.01[b]
TG-D_2O 120 min w pepsin	0.20 ± 0.02 [ab]
TG-D_2O 120 min w/o pepsin	0.23 ± 0.01[b]
TG-H_2O initial gel	0.18 ± 0.01 [a]
TG-H_2O 120 min w pepsin	0.23 ± 0.01[b]
TG-H_2O 120 min w/o pepsin	0.33 ± 0.01[c]

*All values are the mean of triplicate analyses ± the standard deviation. Values marked with different letters in the same column are significantly different across the data set for average area density ($P < 0.01$).

scattering patterns of digesta are provided in Tables 3 and 4. The scattering profiles of casein gels were similar to those reported previously using SAXS and SANS [24,36;40;41;56,65]. However, these studies examined only the intermediate and high q regions and did not characterise the gel structure at low q using ultra-small-angle techniques, which is novel to the current experiment.

3.4.1. Characterisation of the initial casein gel

The spectra of the initial gels (Fig. 7) show the intensity of D_2O gel samples continued to increase with decreasing q-value below 10^{-5} $Å^{-1}$ (higher power law), with a power law exponent for the TG-D_2O and RG-D_2O samples as 1.54 ± 0.02 and 3.31 ± 0.02, respectively. In comparison, the samples prepared in H_2O exhibit a considerably lower power law exponent, with 0.36 ± 0.02 and 0.11 ± 0.02, respectively. The apparent radius of gyration (Rg) for each gel represents the size of micelle aggregates fused together to form the network strands (Table 4). Under these conditions, individual micelles cannot be distinguished from each other, as they would be in solution [100]. The casein micelle aggregates were significantly smaller for TG-D_2O, with a radius of 117 nm, compared to all other samples (147–153 nm). Solvent did not affect the size of the casein micelle aggregates in RG, however the aggregates were larger in H_2O compared to D_2O for TG. This is consistent with previous studies that demonstrate that substitution of H_2O for D_2O can cause a decrease in micelle size due to stronger hydrogen bonding ([29;78], while others have shown no effect [37]).

A more pronounced neutron signal was observed for samples in D_2O in the high q region between 0.01 and 0.1 $Å^{-1}$ compared to those in H_2O (Fig. 7, Fig. 8). The inflection point observed at ~ 0.0 035 $Å^{-1}$ is due to the contrast effect between CCP and protein in the different solvent environments [38], and indicates a less dense internal structure for the H_2O samples also due to weaker hydrogen bonding [20].

3.4.2. Effect of acidification and hydrolysis by pepsin

The effect of the acidic environment of gastric digestion with or without pepsin was investigated using USANS and SANS as a function of time (Fig. 4&8). The power law exponent for region [1] of the scattering pattern is presented in Table 3, where an increase was evident for both the 15 and 120 min digesta compared to the initial gels. However, a significant reduction was measured for the TG samples between the 15 and 120 min time points (with and without pepsin), suggesting a loosening of the gel aggregate microstructure as digestion proceeds after an initial contraction over the first 15 min [70,105].

Table 3
The power law exponent for the initial 10% (w/w) casein gels and their digesta after 15 and 120 min from experiments with and without pepsin and calculated using the ultra-small angle neutron scattering patterns (USANS) at ultra-low q, for the; rennet-induced gel in D_2O (RG-D_2O); rennet-induced gel in H_2O (RG-H_2O); transglutaminase-induced acid gel in D_2O (TG-D_2O) and transglutaminase-induced acid gel in H_2O (TG-H_2O).

		With pepsin		Without pepsin	
Gel type	Initial Gel	15 min	120 min	15 min	120 min
RG-D2O	3.31 ± 0.02 ^{g}	3.85 ± 0.01^{i}	3.58 ± 0.02 ^{h}	3.86 ± 0.01^{i}	3.75 ± 0.01^{hi}
RG-H_2O	0.11 ± 0.02^{a}	3.09 ± 0.03^{e}	2.69 ± 0.03^{d}	3.19 ± 0.03^{ef}	3.11 + 0.02^{ef}
TG-D_2O	1.54 ± 0.02^{c}	4.10 ± 0.03^{j}	2.79 ± 0.03^{d}	3.31 ± 0.03 ^{g}	0.15 ± 0.03^{a}
TG-H_2O	0.36 ± 0.02^{b}	4.24 ± 0.04 ^{k}	4.06 ± 0.05^{j}	4.48 ± 0.08 ^{l}	3.66 ± 0.09 ^{h}

*All values are the mean of single analyses ± the standard deviation of the model fitting. Values marked with a different letter (lower case) across the data set are significantly different across the initial gel samples, and their digesta with and without pepsin at the different time points (P < 0.01).

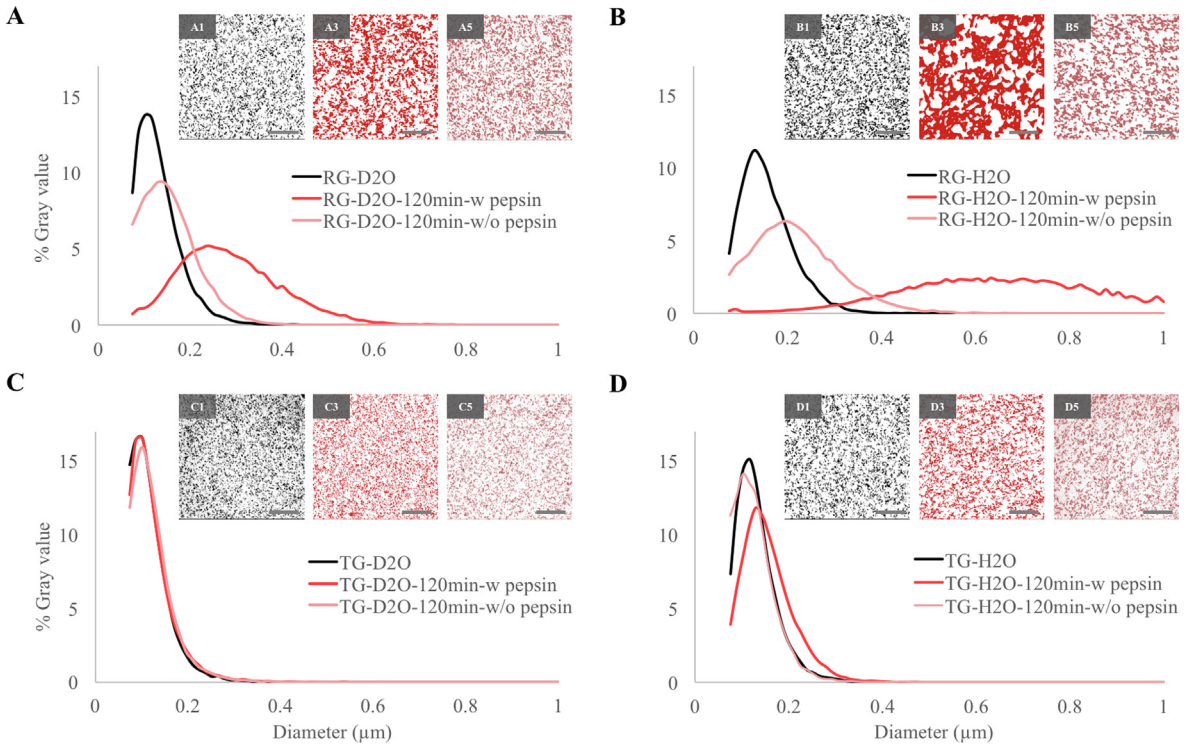

Fig. 5. Partial particle size distribution of the initial 10% (w/w) casein gels and their digesta after 120 min obtained from experiments with (w) and without (w/o) pepsin and calculated using the transmission electron microscopy (TEM) images, for the; (A) rennet-induced gel in D_2O (RG-D_2O); (B) rennet-induced gel prepared in H_2O (RG-H_2O); (C) transglutaminase-induced acid gel in D_2O (TG-D_2O); and (D) transglutaminase-induced acid gel in H_2O (TG-H_2O). The analysis was computed from the average of 10 images per sample. Magnification 1650X; Scale bars represent 5 μm. TEM binary images were color coded relating to the sample.

The size of the individual casein micelle aggregates did not change considerably throughout the experiment with or without pepsin for TG (Table 4), however differing effects were observed for RG. In H_2O, the apparent aggregate size increased from 153 nm to 501 nm with pepsin and 293 nm without pepsin after 15 min. However, the apparent aggregate size decreased significantly between the initial gel and 15 min digesta for RG-D_2O. Across the different gel and solvent combinations, TG-D_2O presents the smallest micelle aggregate size (Table 4), which remained consistently small throughout the experiment with or without pepsin, in agreement with the SEM images.

The inflection at high q (0.0035 $Å^{-1}$) becomes progressively wider with time, both with and without pepsin (Fig. 8). However, the extent of this shift to a higher q value and intensity is greater in samples exposed to acidic conditions without pepsin, compared to those with the enzyme present.

3.5. Soluble protein and α-amino release

To characterize the contribution of the pepsin enzyme towards the structural devolution of RG and TG, the amount of protein degradation after 15 and 120 min was examined by comparing the level of soluble protein in the digesta supernatant to the total protein content, and using an OPA assay to quantify the amount of solubilised low molecular weight peptides (10 kDa) and amino acids. Table 5 A & B shows similar trends in protein degradation using both methods.

As expected, almost no protein degradation and small peptide release were quantified in the supernatants of control samples (without pepsin). However, high levels of protein hydrolysis were measured in the supernatants obtained from gels exposed to the *in vitro* conditions with pepsin, i.e. up to 2.6% solubilised peptides and amino acids and 20% solubilised protein after 120 min.

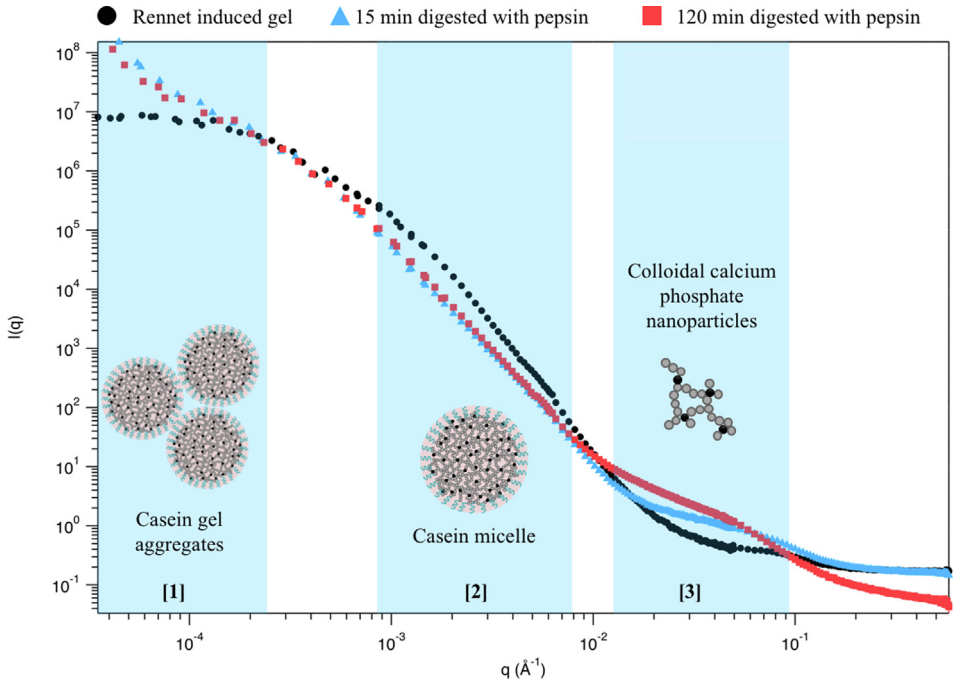

Fig. 6. Schematic representation of the models applied to segments of a combined small angle neutron scattering (SANS) and ultra-small angle neutron scattering (USANS) curve at different size scales used for the present study. The example provided is a rennet-induced gel (RG) and its digesta prepared and digested in H_2O after 15 and 120 min.

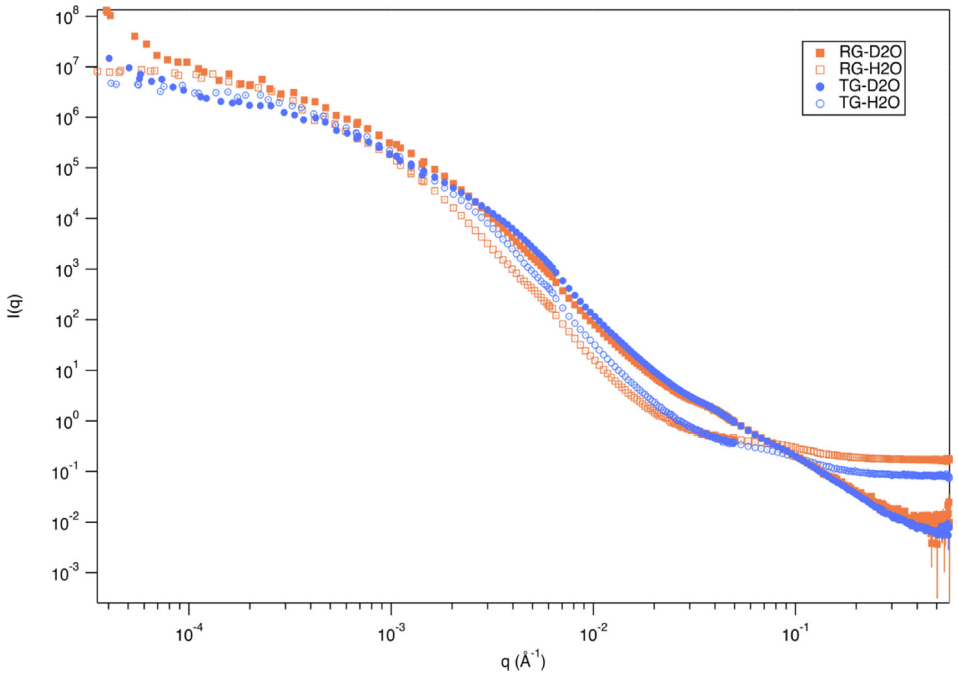

Fig. 7. The small angle neutron scattering (SANS) profiles of the initial 10% (w/w) protein gels of; rennet-induced gel in D_2O (RG-D_2O); rennet-induced gel in H_2O (RG-H_2O); transglutaminase-induced acid gel in D_2O (TG-D_2O); and transglutaminase-induced acid gel in H_2O (TG- H_2O).

4. Discussion

4.1. Characterisation of the initial gel structure

The quantitative characterisation of the RG and TG casein gels prepared in H_2O and D_2O was examined using gelation (Table 1) and small deformation (Fig. 2) rheological measurements, scattering techniques (Tables 3&4, Fig. 8), in combination with SEM (Fig. 4) and TEM (Fig. 5). The gelation kinetics of casein are greatly influenced by factors such as temperature, protein and enzyme concentration[44,67,68,106], and it is difficult to directly compare absolute rheological behaviour across studies. However, in general terms, the literature has shown rennet-induced gels to be stronger than acid gels [57] and transglutaminase acid gels to be significantly firmer than acid gels without transglutaminase treatment ([5,21;30;90]. No direct comparisons between rennet-induced or transglutaminase-induced acid gels are available in the literature at the current time.

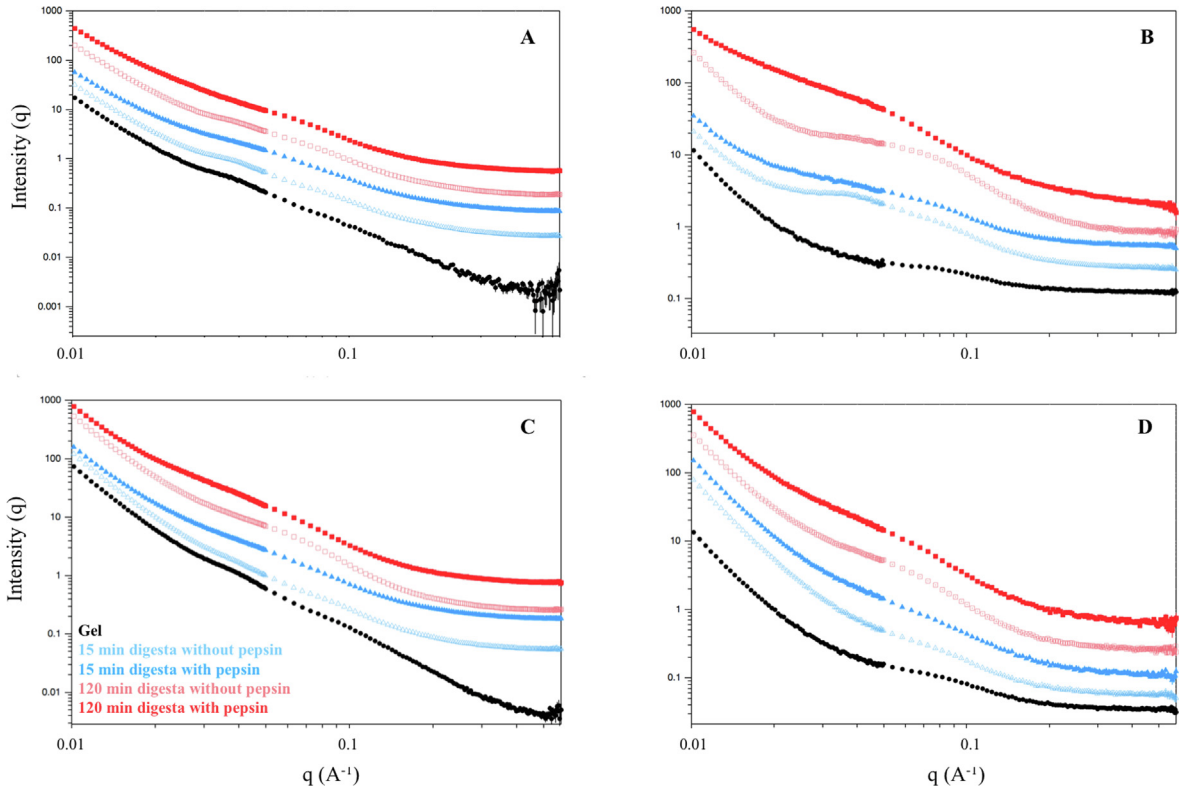

Fig. 8. The high-q region small angle neutron scattering (SANS) profiles of the initial 10%(w/w) protein gels and their digesta after 15 (blue) and 120 min (red) obtained from experiments with and without pepsin, of the; (A) rennet-induced gel in D_2O (RG-D_2O); (B) rennet-induced gel in H_2O (RG-H_2O); (C) transglutaminase-induced acid gel in D_2O (TG-D_2O); and (D) transglutaminase-induced acid gel in H_2O (TG-H_2O). For clarity, SANS patterns reported are shifts in the y-axis direction. (For interpretation of the references to color in this figure legend, the reader is referred to the web version of this article.)

Table 4
The radius of gyration (nm) for the initial 10% (w/w) casein gels and their digesta after 15 and 120 min from experiments with and without pepsin and calculated using the small angle neutron scattering patterns (SANS) across low and mid q , for the; rennet-induced gel in D_2O (RG-D_2O); rennet-induced gel in H_2O (RG- H_2O); transglutaminase-induced acid gel in D_2O (TG- D_2O) and transglutaminase-induced acid gel in H_2O (TG- H_2O).

		With pepsin		Without pepsin	
Gel type	Initial Gel	15 min	120 min	15 min	120 min
RG-D2O	150.1 ± 4.3 ^{cd}	114.0 ± 3.6^{ab}	115.5 ± 3.5^{ab}	100.2 ± 2.8^{a}	158.5 ± 4.3^{d}
RG-H_2O	152.8 ± 6.1^{d}	501.2 ± 3.5 ^{g}	314.0 ± 1.5^{f}	293.0 ± 32.9^{f}	212.0 ± 5.4^{e}
TG-D_2O	116.9 ± 2.3^{abc}	117.3 ± 2.6^{abc}	117.9 ± 3.0^{abc}	117.1 ± 2.1^{abc}	115.8 ± 2.2^{ab}
TG-H_2O	146.6 ± 4.1^{bcd}	139.2 ± 6.7^{bcd}	139.8 ± 7.3^{bcd}	165.3 ± 17.2^{d}	135.0 ± 8.6^{bcd}

*All values are the mean of single analyses ± the standard deviation of the model fitting. Values marked with a different letter across the data set are significantly different across the initial gels and their digesta with and without pepsin at the different time points (P < 0.01).

Table 5
Degree of soluble protein content (%, A) and peptide release (<10 kDa) ratio as measured via an OPA assay (B) of the initial 10% (w/w) protein gels and their digesta after 15 and 120 min obtained from experiments with and without pepsin, of the; rennet-induced gel in D_2O (RG-D_2O); rennet-induced gel in H_2O (RG-H_2O); transglutaminase-induced acid gel in D_2O (TG-D_2O); and transglutaminase-induced acid gel in H_2O (TG-H_2O).

A	With pepsin		Without pepsin	
Gel type	15 min	120 min	15 min	120 min
RG-D2O	9.60 ± 1.33^{f}	21.02 ± 0.02^{i}	3.22 ± 0.11^{ab}	5.67 ± 0.11 ^{cd}
RG-H_2O	8.80 ± 1.99^{ef}	16.86 ± 0.09^{gh}	5.07 ± 0.02^{bc}	7.53 ± 0.05^{def}
TG-D_2O	7.56 ± 0.62^{def}	18.98 ± 0.63^{hi}	1.21 ± 0.02^{a}	2.49 ± 0.45^{a}
TG-H_2O	6.73 ± 0.17^{cde}	16.12 ± 1.00 ^{g}	1.67 ± 0.06^{a}	3.03 ± 1.12^{ab}
B	With pepsin		Without pepsin	
Gel type	15 min	120 min	15 min	120 min
RG-D2O	0.39 ± 0.14^{a}	2.63 ± 0.33^{c}	0.03 ± 0.01^{a}	0.23 ± 0.09^{a}
RG-H_2O	0.52 ± 0.09^{a}	1.60 ± 0.11^{b}	0.08 ± 0.04^{a}	0.05 ± 0.01^{a}
TG-D_2O	1.48 ± 0.68^{b}	1.73 ± 0.27^{b}	0.02 ± 0.01^{a}	0.03 ± 0.01^{a}
TG-H_2O	0.35 ± 0.09^{a}	1.35 ± 0.02^{b}	0.06 ± 0.01^{a}	0.07 ± 0.01^{a}

*Values marked with different letters are significantly different across all samples within each treatment A or B (P < 0.01).

The results of this study demonstrate that the solvent environment greatly contributes to the formation of the gel network matrix. The strength of the hydrophobic interactions between the proteins of a gel formed in D_2O are greater than in the H_2O environment [77] leading to a higher number of aggregates and/or cross-linking junction points (Tables 2&3) and a lower free energy of junction formation. This created a tighter strand network with higher degree of protein–protein interactions. This is supported by the enhanced gel firmness (Table 1), hence decreasing porosity (Fig. 4&5), and consistent with observations for previous gel systems including gelatin and fibrinogen [14,34,43,47,50;77]). These observations were confirmed by TEM where a more homogeneous and narrower distribution of micelle particle size was observed for gels with D_2O compared to H_2O (Fig. 5).

The compactness of gel microstructure appeared more homogeneous in TG while RG illustrates localised dense structures. The finer network observed for TG compared to the coarse structure of RG is likely due to the cross-linking of more neighbouring micelle aggregates at junction points throughout the gel network (Fig. 1&4&5), and supports previous observations by others in TG and RG systems[27]; Færgemand, et al., 1997; [51]. DeKruif, et al. [24] showed that cross linking with transglutaminase did not affect casein micelle size compared to the size of micelles in the original micellar solution. Therefore, the smaller size of micelles found in TG-D_2O (Fig. 5 C) is believed to be due to the rearrangement of internal gaps by the loss of CCP during acidification [19,72,99].

4.1.1. Neutron scattering: A useful tool for the characterisation of gel microstructure

The ultra-low q region [1] allows for the characterisation of micrometre-sized objects, relating to the protein micelle aggregates of the gel structure. To characterise the gel microstructure at this scale, the principles used previously for mass fractal structures have been applied [7,16]. It is proposed that scattering in this region is defined by the compactness of the stranded gel network, made up of spherical casein aggregates that interact with each other. The negative power law exponents of the ultra-low q region (relating to the slope, shown in Table 3) are proportionate to the packing of the protein strands, hence their localised density or compactness within the protein filled regions [105].

The higher negative power law of the D_2O gels indicated a densely packed aggregate network structure, whereas gels formulated with H_2O approached a plateau with decreasing q, indicating a looser and less dense network on a micro-scale (Table 3). This supports the denser microstructure of D_2O observed in SEM and TEM compared to H_2O due to its higher hydrophobicity. Previous studies have shown no differences in casein micelle diameter for solutions prepared in D_2O compared to H_2O [24,38]. The slightly larger casein micelle aggregates obtained with H_2O in our study is supported by the more compact casein precipitate observed by Cuomo, Ceglie, and Lopez [18] and suggests a more pronounced collapse of the hairy hydrophilic κ-casein layer at the surface of the micelle in the more hydrophobic D_2O environment.

The TG samples were expected to have a broader and less intense high-q region compared to RG due to the solubilisation of CCP during the GDL acidification of the casein solution and leading to a disruption of the dense protein regions. However, this did not occur, suggesting that cross-linking by transglutaminase occurs prior to the effect of acidification [79,107].

4.1.2. The breakdown of gel structure during simulated mastication

Dynamic viscoelastic values calculated from the frequency sweep measurements (Fig. 2) are in agreement with the weak gel behaviour observed through the tan δ gelation measurements for both TG and RG samples (Table 1), and is consistent with previous milk gel observations [49;56,62]. The ratio calculated between G′ and frequency is an indication of the tendency for gels to deform upon simulated mastication when placed in the mouth at pH 7, and higher for RG (~0.17) compared to TG (~0.13) prepared using both H_2O and D_2O (Fig. 2). This indicates the higher mechanical strength and elasticity of RG is related to the deformability of the gel in response to shear of mixing [89]. This was also supported by the difference in gel particle size observed for masticated samples entering the stomach vessel after the simulated oral phase, where a higher number of larger particles were observed for RG with no medium sized particles in RG-H_2O (Fig. 3).

4.2. Effect of acidification by simulated gastric fluid and hydrolysis by pepsin

A range of changes were observed in the network structure of both the TG and RG gels when exposed to the simulated acidic environment of the stomach, with and without pepsin. The strong change in gel structure after 15 min with and without pepsin, indicate that structural change occurs almost immediately upon exposure to the acidic environment of the stomach.

The structure present in the initial RG and TG samples develops into heavily compact protein strands as *in vitro* digestion proceeds, yielding a higher negative power law exponent (Fig. 4&5, Table 3). However, comparatively, the localised areas of densely packed strands in RG resulted in higher porosity and increased apparent aggregate size within the network compared to TG, where RG was found to be especially sensitive to the acidic environment of the stomach, promoting gel particle contraction (Fig. 4). These results are in agreement with Barbé, et al. [8], Floury, et al. [33], where rennet-induced gels were observed to undergo a strong contraction once exposed to an acidic environment. This increase in micelle aggregates particle sizing (Fig. 5) and average area density (Table 2) is consistent with a higher sensitivity to the acidic environment. While the compactness of the gel network strands remains within a relatively narrow range from 15 to 120 min, the casein micelle size for RG increases considerably when pepsin is present (Fig. 5. A& B). This indicates that pepsin contributes to the loosening of casein proteins within the micelle structure, creating larger channels into the micelle interior, further accelerating enzyme diffusion and protein hydrolysis [64,96]. This is in agreement with the more pronounced changes observed for the scattering pattern of RG-H_2O after 15 min of *in vitro* gastric digestion with decrease in intensity of the ultra-low q region by a factor of 10, and a decrease by a factor of at least two at high q. Evidence to also support this behaviour is through the greater structural change observed in RG-H_2O and its digesta with large aggregate clusters and pores using SEM and TEM microscopy, and the higher level of solubilised protein, smaller peptides and amino acids measured in the supernatant of RG digesta with pepsin present. Without pepsin, there was no change in casein particle size in RG-D_2O (Fig. 5 C) and only a slight change in RG-H_2O (Fig. 5 D). Despite the higher number of larger gel particles entering the stomach following mastication and the higher gel strength, the porous microstructure of RG provided a larger surface area and thus higher simulated digestibility compared to TG.

In contrast, less significant structural changes were observed between TG samples using SEM (Fig. 4 C1-D5), suggesting the difference in pH between the initial gel and the gastric environment plays a key role [8,69]. In the current study, the pH of RG was ~ pH 6.1 (D_2O) and 6.5 (H_2O) compared to ~ pH 5.7 for TG. The subsequent difference between the initial gel pH and the simulated gastric environment (pH 3) was larger for the RG samples, leading to the observed contraction in gel structure, syneresis and expulsion of solvent from within the gel. After the initial increase in gel packing density and casein micelle aggregate size

observed for TG after 15 min with pepsin, parameters were again reduced by the 120 min mark. This decrease in gel compactness for TG from 15 to 120 min with and without pepsin indicates the effect of the shear of mixing and the subsequent physical disruption at a micro-level. The casein micelles of the TG samples did not tend to swell with or without pepsin (Fig. 5) and no dissolution of CCP particles was observed (Fig. 7) due to the inter- and intramolecular lysine bonds formed by transglutaminase, which aligns with the fact that cross-linking prevents shrinking or swelling of casein micelle to a great extent [94] (Fig. 5 C,D).

The TG structure, on a nano- to micro-scale, appears to be resistant to change from exposure to *in vitro* gastric conditions with pepsin, however the level of solubilised protein, peptides and amino acids are only slightly lower than RG after 120 min (Table 5). This suggests that pepsin has a limited effect on the degradation of the TG structure as the diffusion of pepsin inside the TG particle is limited due to the fine stranded protein network, effectively reducing accessibility of pepsin to the substrate [33]. Coupled with observations that show the formation of progressively smaller gel pieces in the stomach vessel over time, these results suggest the primary cause of TG degradation is due to surface erosion of the gel as opposed to protein hydrolysis and that the degree of digestion is proportional to the size and number of larger gel particles entering the stomach. In addition, cross-linking may increase the resistance to pepsin penetration, hence digestion [73].

Gels formed in D_2O have a finer network and brittle structure compared to H_2O, which suggests the first step of mechanical breakdown will allow hydrolysis to occur on a larger surface area of the smaller, fractured particles. The higher degree of protein degradation for gels in D_2O compared to gels in H_2O, is likely due to differences in gel brittleness. That is, the firmer gels prepared with D_2O (Table 1) have shorter protein strands between the increased number of protein aggregates or cross linking junctions of the D_2O gels (Fig. 4 A1-D1) and leads to a lower yield stress that are less likely to flex with the application of force and shear during the *in vitro* gastric digestion protocol [34,47,50;77;83]. The brittle structure is further confirmed by the higher number of medium-sized particles with gels made in D_2O as opposed to H_2O (Fig. 3). This exposes a greater surface action by pepsin enzyme, hence increasing the degree of overall protein degradation.

5. Conclusion

This study is the first to report the characterisation of gel structure during digestion of casein gels using USANS and SANS. A control experiment without pepsin allowed for the effect of pepsin alone to be distinguished from that of acidification and mixing, and will contribute to the previous studies on the effect of the acidic gastric environment on casein gel properties. In addition, this is the first study to examine a gel prepared and digested in D_2O compared to the equivalent gel prepared in H_2O. While previous work has shown D_2O substitution to result in smaller micelles compared to H_2O in solution, it has been assumed that replacing hydrogen with deuterium in neutron scattering investigations would not influence gel formation and other structural elements within the gel protein network. However, this study highlights that D_2O, commonly used in neutron scattering experiments, markedly affects the gel microstructure and mechanical properties of casein gels. Due to the stabilising effect of D_2O on proteins, and the denser structure of gels observed using SEM and TEM, a lower degree of hydrolysis was expected. However, the digestibility analysis for solubilized protein, peptides and amino acids released through protein hydrolysis were higher in D_2O gels compared to H_2O gels, due to the more brittle structure of the gels, leading to a greater fracturability (Table 5). The differences in gel disintegration and digestibility should be taken into consideration when using D_2O to prepare, characterise and interpret changes in gel structure in future work.

The difference in digestibility observed in this study are driven by a combination of solvent type (H_2O and D_2O) and gel type (RG and TG). The RG-H_2O structure is most affected by the acidic environment; the packing of the protein strands within the digesta is more compact in localised areas, and casein micelles are larger, compared to TG-D_2O. The local compactness of the RG-H_2O gel consequently drives the porosity and pepsin accessibility, while the higher gel firmness does not allow the gel to be affected by mechanical shear during digestion as much. These findings suggest that the gel disintegration observed in the earlier stages of gastric digestion is driven by both mechanical stress and the sensitivity of the casein micelle structure to acidification.

The effect of pepsin instead occurs more readily in the latter stage of gastric digestion, where efficacy is influenced by the ability of the enzyme to penetrate the interior of the gel network. The relationship between digestibility and pepsin action during gastric digestion, hence the ability of pepsin to access the interior of the gel particles, is supported by the results presented herein, where more porous RG gels with larger surface area expressed higher digestibility compared to a finer TG and highly crosslinked network. The initial compactness of the network strands was also influenced by the pH of the initial gel sample itself, which in turn affects the gel microstructure, hence pepsin accessibility. In order to understand this complex digestion process, the influence of different physiological parameters should be taken into account. Future prospects of the work would allow for the effect of the pepsin enzyme diffusion to be unravelled.

CRediT authorship contribution statement

Meltem Bayrak: Conceptualization, Methodology, Investigation, Formal analysis, Writing - original draft. **Jitendra Mata:** Conceptualization, Supervision, Methodology, Validation, Writing - review & editing. **Jared K. Raynes:** Methodology, Validation. **Mark Greaves:** Investigation, Methodology, Validation. **Jacinta White:** Investigation, Methodology, Validation. **Charlotte E. Conn:** Conceptualization, Supervision, Methodology, Validation, Writing - review & editing. **Juliane Floury:** Conceptualization, Supervision, Methodology, Validation, Writing - review & editing. **Amy Logan:** Conceptualization, Supervision, Methodology, Validation, Writing - review & editing.

Declaration of Competing Interest

The authors declare that they have no known competing financial interests or personal relationships that could have appeared to influence the work reported in this paper.

Acknowledgements

We acknowledge the support of the Australian Nuclear Science and Technology Organization (ANSTO) in providing USANS and SANS beam facilities (proposal no. 7399) used in this work. The authors would like to thank AINSE Limited for providing financial assistance (Award - PGRA) to enable work on QUOKKA and KOOKABURRA. The authors thank Jonathan Thévenot (INRAE-STLO) for providing FIJI macro for automatised image analysis. The authors also acknowledge the advice provided by Allison Williams and Roderick Williams (CSIRO Agriculture and Food) during the digestion experiments. Charlotte E. Conn was the recipient of an RMIT Vice Chancellor's Senior Research Fellowship.

References

[1] M.D. Abràmoff, P.J. Magalhães, S.J. Ram, Image processing with ImageJ, Biophoton. Int. 11 (7) (2004) 36–42.
[2] J. Adler-Nissen, Enzymic hydrolysis of food proteins: Elsevier applied science publishers (1986).
[3] J.M. Aguilera, Why food microstructure?, J. Food Eng. 67 (1–2) (2005) 3–11.
[4] S. Aime, L. Cipelletti, L. Ramos, Power law viscoelasticity of a fractal colloidal gel, J. Rheol. 62 (6) (2018) 1429–1441.
[5] S. Anema, S. Lauber, S.K. Lee, T. Henle, H. Klostermeyer, Rheological properties of acid gels prepared from pressure-and transglutaminase-treated skim milk, Food Hydrocolloids 19 (5) (2005) 879–887.
[6] S. Anema, D. Pinder, R. Hunter, Y. Hemar, Effects of storage temperature on the solubility of milk protein concentrate (MPC85), Food Hydrocolloids 20 (2–3) (2006) 386–393.
[7] H.D. Bale, P.W. Schmidt, Small-angle X-ray-scattering investigation of submicroscopic porosity with fractal properties, Phys. Rev. Lett. 53 (6) (1984) 596.
[8] F. Barbé, O. Ménard, Y. Le Gouar, C. Buffière, M.-H. Famelart, B. Laroche, S. Le Feunteun, D. Rémond, D. Dupont, Acid and rennet gels exhibit strong differences in the kinetics of milk protein digestion and amino acid bioavailability, Food Chem. 143 (2014) 1–8.
[9] R. Bhattacharya, S. Saha, O. Kostina, L. Muravnik, A. Mitra, Replacing critical point drying with a low-cost chemical drying provides comparable surface image quality of glandular trichomes from leaves of Millingtonia hortensis L. f. in scanning electron micrograph (2020).
[10] G.M. Bornhorst, O. Gouseti, M.S. Wickham, S. Bakalis, Engineering digestion: multiscale processes of food digestion, J. Food Sci. 81 (3) (2016) R534–R543.
[11] A. Bouchoux, G. Gesan-Guiziou, J. Pérez, B. Cabane, How to squeeze a sponge: casein micelles under osmotic stress, a SAXS study, Biophys. J .. 99 (11) (2010) 3754–3762.
[12] L.G. Bremer, T. van Vliet, P. Walstra, Theoretical and experimental study of the fractal nature of the structure of casein gels, J. Chem. Soc., Faraday Trans. 1 F 85 (10) (1989) 3359–3372.
[13] A. Brodkorb, L. Egger, M. Alminger, P. Alvito, R. Assunção, S. Ballance, T. Bohn, C. Bourlieu-Lacanal, R. Boutrou, F. Carrière, INFOGEST static in vitro simulation of gastrointestinal food digestion, Nat. Protoc. 14 (4) (2019) 991.
[14] M.V.C. Cardoso, E. Sabadini, The gelling of κ-carrageenan in light and heavy water, Carbohydr. Res. 345 (16) (2010) 2368–2373.
[15] J. Chandrapala, G.J. Martin, S.E. Kentish, M. Ashokkumar, Dissolution and reconstitution of casein micelle containing dairy powders by high shear using ultrasonic and physical methods, Ultrason. Sonochem. 21 (5) (2014) 1658–1665.
[16] A.Y. Cherny, E. Anitas, V. Osipov, A. Kuklin, Scattering from surface fractals in terms of composing mass fractals, J. Appl. Crystallogr. 50 (3) (2017) 919–931.
[17] A.K. Covington, M. Paabo, R.A. Robinson, R.G. Bates, Use of the glass electrode in deuterium oxide and the relation between the standardized pD (paD) scale and the operational pH in heavy water, Anal. Chem. 40 (4) (1968) 700–706.
[18] F. Cuomo, A. Ceglie, F. Lopez, Temperature dependence of calcium and magnesium induced caseinate precipitation in H2O and D2O, Food Chem. 126 (1) (2011) 8–14.
[19] D.G. Dalgleish, A.J. Law, pH-induced dissociation of bovine casein micelles. I. Analysis of liberated caseins, J. Dairy Res. 55 (4) (1988) 529–538.
[20] L. Day, J. Raynes, A. Leis, L. Liu, R. Williams, Probing the internal and external micelle structures of differently sized casein micelles from individual cows milk by dynamic light and small-angle X-ray scattering, Food Hydrocolloids 69 (2017) 150–163.
[21] C.K. de Kruif, S.G. Anema, C. Zhu, P. Havea, C. Coker, Water holding capacity and swelling of casein hydrogels, Food Hydrocolloids 44 (2015) 372–379.
[22] C. DeKruif, Casein micelles: diffusivity as a function of renneting time, Langmuir 8 (12) (1992) 2932–2937.
[23] C. DeKruif, C. Holt, Casein micelle structure, functions and interactions. In *Advanced dairy chemistry—1 proteins*, Springer, 2003, pp. 233–276.
[24] C. DeKruif, T. Huppertz, V.S. Urban, A.V. Petukhov, Casein micelles and their internal structure, Adv. Colloid Interface Sci. 171 (2012) 36–52.
[25] C. DeKruif, E.B. Zhulina, κ-casein as a polyelectrolyte brush on the surface of casein micelles, Colloids Surf. A 117 (1–2) (1996) 151–159.
[26] E. Dickinson, Structure formation in casein-based gels, foams, and emulsions, Colloids Surf. A 288 (1–3) (2006) 3–11.
[27] J. Domagała, D. Najgebauer-Lejko, I. Wieteska-Śliwa, M. Sady, M. Wszołek, G. Bonczar, M. Filipczak-Fiutak, Influence of milk protein cross-linking by transglutaminase on the rennet coagulation time and the gel properties, J. Sci. Food Agric. 96 (10) (2016) 3500–3507.
[28] M. Doucet, S. King, P. Butler, P. Kienzle, P. Parker, J. Krzywon, A. Jackson, T. Richter, M. Gonzales, T. Nielsen, SasView, Version In. 5 (2019).
[29] Ericsson, C. A., Söderman, O., Garamus, V. M., Bergström, M., & Ulvenlund, S., Effects of temperature, salt, and deuterium oxide on the self-aggregation of alkylglycosides in dilute solution. 1. n-nonyl-β-D-glucoside. Langmuir, 20 (4) (2004) 1401–1408.
[30] M. Færgemand, K. Qvist, Transglutaminase: effect on rheological properties, microstructure and permeability of set style acid skim milk gel, Food Hydrocolloids 11 (3) (1997) 287–292.
[31] J. Feher, Digestion and absorption of the macronutrients, Quantit. Hum. Physiol. 731 (2012).
[32] J. Finnigan, D. Jacobs, Light scattering by ellipsoidal particles in solution, J. Phys. D Appl. Phys. 4 (1) (1971) 72.
[33] J. Floury, T. Bianchi, J. Thévenot, D. Dupont, F. Jamme, E. Lutton, M. Panouillé, F. Boué, S. Le Feunteun, Exploring the breakdown of dairy protein gels during in vitro gastric digestion using time-lapse synchrotron deep-UV fluorescence microscopy, Food Chem. 239 (2018) 898–910.
[34] W. Gadomski, B. Ratajska-Gadomska, M. Boniecki, Time evolution of the Raman and fluorescence spectra of the D2O and H2O gelatin solutions during the sol–gel transition, J. Mol. Struct. 511 (1999) 181–187.
[35] A. Guinier, G. Fournet, K.L. Yudowitch, Small-angle scattering of X-rays (1955).
[36] S. Hansen, R. Bauer, S.B. Lomholt, K.B. Quist, J.S. Pedersen, K. Mortensen, Structure of casein micelles studied by small-angle neutron scattering, Eur. Biophys. J. 24 (3) (1996) 143–147.
[37] L. He, V.M. Garamus, S.S. Funari, M. Malfois, R. Willumeit, B. Niemeyer, Comparison of small-angle scattering methods for the structural analysis of octyl-β-maltopyranoside micelles, J. Phys. Chem. B 106 (31) (2002) 7596–7604.
[38] C. Holt, C. De Kruif, R. Tuinier, P. Timmins, Substructure of bovine casein micelles by small-angle X-ray and neutron scattering, Colloids Surf. A 213 (2–3) (2003) 275–284.
[39] D.S. Horne, Casein micelle structure: models and muddles, Curr. Opin. Colloid Interface Sci. 11 (2–3) (2006) 148–153.
[40] T. Huppertz, C.G. DeKruif, Structure and stability of nanogel particles prepared by internal cross-linking of casein micelles, Int. Dairy J. 18 (5) (2008) 556–565.
[41] B. Ingham, A. Smialowska, G.D. Erlangga, L. Matia-Merino, N. Kirby, C. Wang, R.G. Haverkamp, A. Carr, Revisiting the interpretation of casein micelle SAXS data, Soft Matter 12 (33) (2016) 6937–6953.
[42] D. Jaros, U. Schwarzenbolz, N. Raak, J. Löbner, T. Henle, H. Rohm, Cross-linking with microbial transglutaminase: Relationship between polymerisation degree and stiffness of acid casein gels, Int. Dairy J. 38 (2) (2014) 174–178.
[43] L. Jean, C.F. Lee, P. Hodder, N. Hawkins, D.J. Vaux, Dynamics of the formation of a hydrogel by a pathogenic amyloid peptide: islet amyloid polypeptide, Sci. Rep. 6 (2016) 32124.
[44] A.O. Karlsson, R. Ipsen, Y. Ardö, Rheological properties and microstructure during rennet induced coagulation of UF concentrated skim milk, Int. Dairy J. 17 (6) (2007) 674–682.
[45] S.R. Kline, Reduction and analysis of SANS and USANS data using IGOR Pro, J. Appl. Crystallogr. 39 (6) (2006) 895–900.
[46] F. Kong, R.P. Singh, Disintegration of solid foods in human stomach, J. Food Sci. 73 (5) (2008) R67–R80.
[47] G.C. Kresheck, H. Schneider, H.A. Scheraga, The Effect of D2O on the Thermal Stability of Proteins. Thermodynamic Parameters for the Transfer of Model Compounds from H2O to D2O1, 2, J. Phys. Chem. 69 (9) (1965) 3132–3144.
[48] S. Laiho, R.P. Williams, A. Poelman, I. Appelqvist, A. Logan, Effect of whey protein phase volume on the tribology, rheology and sensory properties of fat-free stirred yoghurts, Food Hydrocolloids 67 (2017) 166–177.
[49] R. Lapasin, S. Pricl, Rheology of polysaccharide systems, in: Rheology of industrial polysaccharides: Theory and applications, Springer, 1995, pp. 250–494.
[50] U. Larsson, Polymerization and gelation of fibronogen in D2O, Eur. J. Biochem. 174 (1) (1988) 139–144.
[51] S.Y. Lee, M.-J. Choi, H.-Y. Cho, M. Davaatseren, Effects of High-Pressure, Microbial Transglutaminase and Glucono-δ-Lactone on the Aggregation Properties of Skim Milk, Korean J. Food Sci. Anim. Resour. 36 (3) (2016) 335.
[52] D. Legland, I. Arganda-Carreras, P. Andrey, MorphoLibJ: integrated library and plugins for mathematical morphology with ImageJ, Bioinformatics 32 (22) (2016) 3532–3534.
[53] D. Legland, J. Beaugrand, Automated clustering of lignocellulosic fibres based on morphometric features and using clustering of variables, Ind. Crops Prod. 45 (2013) 253–261.
[54] D. Legland, M.F. Devaux, B. Bouchet, F. Guillon, M. Lahaye, Cartography of cell morphology in tomato pericarp at the fruit scale, J. Microsc. 247 (1) (2012) 78–93.
[55] Q. Li, Z. Zhao, Acid and rennet-induced coagulation behavior of casein micelles with modified structure, Food Chem. (2019).
[56] Z. Li, Z. Yang, D. Otter, C. Rehm, N. Li, P. Zhou, Y. Hemar, Rheological and structural properties of coagulated milks reconstituted in D2O: Comparison between rennet and a tamarillo enzyme (tamarillin), Food Hydrocolloids 79 (2018) 170–178.
[57] X. Liu, H. Zhang, F. Wang, J. Luo, H. Guo, F. Ren, Rheological and structural properties of differently acidified and renneted milk gels, J. Dairy Sci. 97 (6) (2014) 3292–3299.
[58] A. Logan, L. Day, A. Pin, M. Auldist, A. Leis, A. Puvanenthiran, M.A. Augustin, Interactive effects of milk fat globule and casein micelle size on the renneting properties of milk, Food Bioprocess Technol. 7 (11) (2014) 3175–3185.
[59] A. Logan, A. Leis, L. Day, S.K. Øiseth, A. Puvanenthiran, M.A. Augustin, Rennet gelation properties of milk: Influence of natural variation in milk fat globule size and casein micelle size, Int. Dairy J. 46 (2015) 71–77.
[60] L. Lorieau, A. Halabi, A. Ligneul, E. Hazart, D. Dupont, J. Floury, Impact of the dairy product structure and protein nature on the proteolysis and amino acid bioaccessiblity during in vitro digestion, Food Hydrocolloids 82 (2018) 399–411.
[61] C. Loupiac, How neutron scattering experiments can target the structure and dynamics of milk proteins?, Curr Opin. Food Sci. 9 (2016) 93–97.

[62] J.A. Lucey, Formation and physical properties of milk protein gels, J. Dairy Sci. 85 (2) (2002) 281–294.
[63] J.A. Lucey, Milk protein gels, in: Milk proteins, Elsevier, 2020, pp. 599–632.
[64] Q. Luo, J.W. Borst, A.H. Westphal, R.M. Boom, A.E. Janssen, Pepsin diffusivity in whey protein gels and its effect on gastric digestion, Food Hydrocolloids 66 (2017) 318–325.
[65] J.P. Mata, P. Udabage, E.P. Gilbert, Structure of casein micelles in milk protein concentrate powders via small angle X-ray scattering, Soft Matter 7 (8) (2011) 3837–3843.
[66] D.J. McClements, E.A. Decker, Y. Park, J. Weiss, Designing food structure to control stability, digestion, release and absorption of lipophilic food components, Food Biophys. 3 (2) (2008) 219–228.
[67] M. Mellema, J. Heesakkers, J. Van Opheusden, T. Van Vliet, Structure and scaling behavior of aging rennet-induced casein gels examined by confocal microscopy and permeametry, Langmuir 16 (17) (2000) 6847–6854.
[68] M. Mellema, P. Walstra, J. Van Opheusden, T. Van Vliet, Effects of structural rearrangements on the rheology of rennet-induced casein particle gels, Adv. Colloid Interface Sci. 98 (1) (2002) 25–50.
[69] Y.A. Mennah-Govela, G.M. Bornhorst, Food buffering capacity: quantification methods and its importance in digestion and health, Food Funct. (2020).
[70] D. Mildner, P. Hall, Small-angle scattering from porous solids with fractal geometry, J. Phys. D Appl. Phys. 19 (8) (1986) 1535.
[71] A. Mimouni, H.C. Deeth, A.K. Whittaker, M.J. Gidley, B.R. Bhandari, Rehydration process of milk protein concentrate powder monitored by static light scattering, Food Hydrocolloids 23 (7) (2009) 1958–1965.
[72] C. Moitzi, A. Menzel, P. Schurtenberger, A. Stradner, The pH induced sol– gel transition in skim milk revisited. A detailed study using time-resolved light and X-ray scattering experiments, Langmuir 27 (6) (2011) 2195–2203.
[73] E. Monogioudi, G. Faccio, M. Lille, K. Poutanen, J. Buchert, M.-L. Mattinen, Effect of enzymatic cross-linking of β-casein on proteolysis by pepsin, Food Hydrocolloids 25 (1) (2011) 71–81.
[74] P. Nielsen, D. Petersen, C. Dambmann, Improved method for determining food protein degree of hydrolysis, J. Food Sci. 66 (5) (2001) 642–646.
[75] J.E. Norton, G.A. Wallis, F. Spyropoulos, P.J. Lillford, I.T. Norton, Designing food structures for nutrition and health benefits, Ann. Rev. Food Sci. Technol. 5 (2014) 177–195.
[76] J. O'Mahony, J. Lucey, P. McSweeney, Chymosin-mediated proteolysis, calcium solubilization, and texture development during the ripening of Cheddar cheese, J. Dairy Sci. 88 (9) (2005) 3101–3114.
[77] D. Oakenfull, A. Scott, Gelatin gels in deuterium oxide, Food Hydrocolloids 17 (2) (2003) 207–210.
[78] T. Ozawa, T. Asakawa, V.M. Garamus, A. Ohta, S. Miyagishi, Effect of D2O Solvent on the Micellization Behavior of 2-Hydroxy-1, 1, 2, 3, 3-pentahydroperfluoroundecyldiethyl-ammonium Halides, J. Oleo Sci. 54 (11) (2005) 585–588.
[79] B. Ozer, H.A. Kirmaci, S. Oztekin, A. Hayaloglu, M. Atamer, Incorporation of microbial transglutaminase into non-fat yogurt production, Int. Dairy J. 17 (3) (2007) 199–207.
[80] J. Parada, J. Aguilera, Food microstructure affects the bioavailability of several nutrients, J. Food Sci. 72 (2) (2007) R21–R32.
[81] J. Pasquier, A. Brûlet, A. Boire, F. Jamme, J. Perez, T. Bizien, E. Lutton, F. Boué, Monitoring food structure during digestion using small-angle scattering and imaging techniques, Colloids Surf. A 570 (2019) 96–106.
[82] L.G. Phillips, Structure-function properties of food proteins, Academic Press, 2013.
[83] A. Puvanenthiran, R. Williams, M. Augustin, Structure and visco-elastic properties of set yoghurt with altered casein to whey protein ratios, Int. Dairy J. 12 (4) (2002) 383–391.
[84] G. Quaglia, L. Gennaro, ENZYMES| Uses in Food Processing (2003).
[85] N. Raak, H. Rohm, D. Jaros, Cross-linking with microbial transglutaminase: Isopeptide bonds and polymer size as drivers for acid casein gel stiffness, Int. Dairy J. 66 (2017) 49–55.
[86] N. Raak, H. Rohm, D. Jaros, Enzymatic cross-linking of casein facilitates gel structure weakening induced by overacidification, Food Biophys. 12 (2) (2017) 261–268.
[87] C. Rehm, A. Brûlé, A.K. Freund, S.J. Kennedy, Kookaburra: the ultra-small-angle neutron scattering instrument at OPAL, J. Appl. Crystallogr. 46 (6) (2013) 1699–1704.
[88] E. Rose, Factors influencing gastric emptying, J. Forensic Sci. 24 (1) (1979) 200–206.
[89] E. Sabadini, M. Hubinger, R. Cunha, The effects of sucrose on the mechanical properties of acid milk proteins-kappa-carrageenan gels, Braz. J. Chem. Eng. 23 (1) (2006) 55–65.
[90] C. Schorsch, H. Carrie, I. Norton, Cross-linking casein micelles by a microbial transglutaminase: influence of cross-links in acid-induced gelation, Int. Dairy J. 10 (8) (2000) 529–539.
[91] R.M. Shah, J.P. Mata, G. Bryant, L. de Campo, A. Ife, A.V. Karpe, S.R. Jadhav, D.S. Eldridge, E.A. Palombo, I.H. Harding, Structure Analysis of Solid Lipid Nanoparticles for Drug Delivery: A Combined USANS/SANS Study, Part. Part. Syst. Char. 36 (1) (2019) 1800359.
[92] J. Silva, D. Legland, C. Cauty, I. Kolotuev, J. Floury, Characterization of the microstructure of dairy systems using automated image analysis, Food Hydrocolloids 44 (2015) 360–371.
[93] N. Silva, F. Casanova, F. Gaucheron, A.V.N. de Carvalho Teixeira, G.M. da Silva, L.A. Minim, A.F. De Carvalho, Combined effect of transglutaminase and sodium citrate on the microstructure and rheological properties of acid milk gel, Food Hydrocolloids 82 (2018) 304–311.
[94] M. Smiddy, J.-E. Martin, A. Kelly, C. De Kruif, T. Huppertz, Stability of casein micelles cross-linked by transglutaminase, J. Dairy Sci. 89 (6) (2006) 1906–1914.
[95] G. Somaratne, M.J. Ferrua, A. Ye, F. Nau, J. Floury, D. Dupont, J. Singh, Food material properties as determining factors in nutrient release during human gastric digestion: a review, Crit. Rev. Food Sci. Nutr. (2020) 1–17.
[96] J. Thevenot, C. Cauty, D. Legland, D. Dupont, J. Floury, Pepsin diffusion in dairy gels depends on casein concentration and microstructure, Food Chem. 223 (2017) 54–61.
[97] M. Tunick, Rheology of dairy foods that gel, stretch, and fracture, J. Dairy Sci. 83 (8) (2000) 1892–1898.
[98] S.L. Turgeon, L.-E. Rioux, Food matrix impact on macronutrients nutritional properties, Food Hydrocolloids 25 (8) (2011) 1915–1924.
[99] A.M. Van Hooydonk, H. Hagedoorn, I. Boerrigter, pH-induced physico-chemical changes of casein micelles in milk and their effect on renneting. 1. Effect of acidification on physico-chemical properties, Netherlands Milk Dairy J. 40 (2–3) (1986) 281–296.
[100] T. van Vliet, C.M. Lakemond, R.W. Visschers, Rheology and structure of milk protein gels, Curr. Opin. Colloid Interface Sci. 9 (5) (2004) 298–304.
[101] A.J. Vasbinder, A.C. Alting, R.W. Visschers, C.G. DeKruif, Texture of acid milk gels: formation of disulfide cross-links during acidification, Int. Dairy J. 13 (1) (2003) 29–38.
[102] J.F. White, J.A. Werkmeister, S.L. Hilbert, J.A. Ramshaw, Heart valve collagens: cross-species comparison using immunohistological methods, J. Heart Valve Dis. 19 (6) (2010) 766.
[103] K. Wood, J.P. Mata, C.J. Garvey, C.-M. Wu, W.A. Hamilton, P. Abbeywick, D. Bartlett, F. Bartsch, P. Baxter, N. Booth, QUOKKA, the pinhole small-angle neutron scattering instrument at the OPAL Research Reactor, Australia: design, performance, operation and scientific highlights, J. Appl. Crystallogr. 51 (2) (2018) 294–314.
[104] R.Y. Yada, Proteins in food processing, Woodhead Publishing, 2017.
[105] L. Yu, G.E. Yakubov, E.P. Gilbert, K. Sewell, A.M. van de Meene, J.R. Stokes, Multi-scale assembly of hydrogels formed by highly branched arabinoxylans from Plantago ovata seed mucilage studied by USANS/SANS and rheology, Carbohydr. Polym. 207 (2019) 333–342.
[106] Q. Zhong, C.R. Daubert, O.D. Velev, Physicochemical variables affecting the rheology and microstructure of rennet casein gels, J. Agric. Food Chem. 55 (7) (2007) 2688–2697.
[107] M. Ziarno, D. Zaręba, The effect of the addition of microbial transglutaminase before the fermentation process on the quality characteristics of three types of yogurt, Food Sci. Biotechnol. 29 (1) (2020) 109–119.